THOR abdomen prototype finite element model development and validation

Contents

2.1 Introduction

A finite element model of the THOR dummy has been developed by NHTSA. The validation of this model under impact conditions needs to be confirmed, especially for the abdomen region with regards to loading velocity dependency. The validation regarding test data should be assessed for both impactor and seatbelt loading cases. In order to be able to reproduce a variety of test configurations, the prototype abdomen described in Compigne et al. 2015 should also be available as a finite element model, including the APTS sensors, and validated against test data. Recently performed tests from NHTSA's VRTC [1] on this prototype abdomen provide data for validation. Once the validation versus test data will be assessed, the prototype abdomen model could be used to propose design changes or material modifications in order to improve its biofidelity.

2.2 Finite element model of the THOR abdomen

A finite element model of the THOR dummy under LS-DYNA has been developed since 2000 by NHTSA and other partners. The version 2.0.5 model of the Mod-kit dummy was used. The model is described in THOR FE [2] Manual (Panzer et al. 2015). The model has been built using CAD [3] drawings of the dummy. It contains 469 parts, approximately 460 000 elements and 237 000 nodes. Rigid and deformable material properties derived from impact test data are used. Figure 2.1a shows a global view of the dummy model.

Figure 2.1b shows the upper and lower abdomen of the dummy model. Both abdomens consist in a front and a rear foam block, linked to a plate attached to the dummy spine. Tables 2.1 shows the properties of the main deformable parts of the dummy abdomen and pelvis. According to GESAC, Inc. 1999, the front foam material is an open cell charcoal polyester and the rear foam material is a closed cell sponge rubber. Figure 2.2 shows the material curves associated with the upper and lower abdomen parts for different strain rates. These curves are used for hyperelastic material models that allow strain rate dependency (`MAT_057: LOW_DENSITY_FOAM` and `MAT_083: FU_CHANG_FOAM`, detailed in Appendix C).

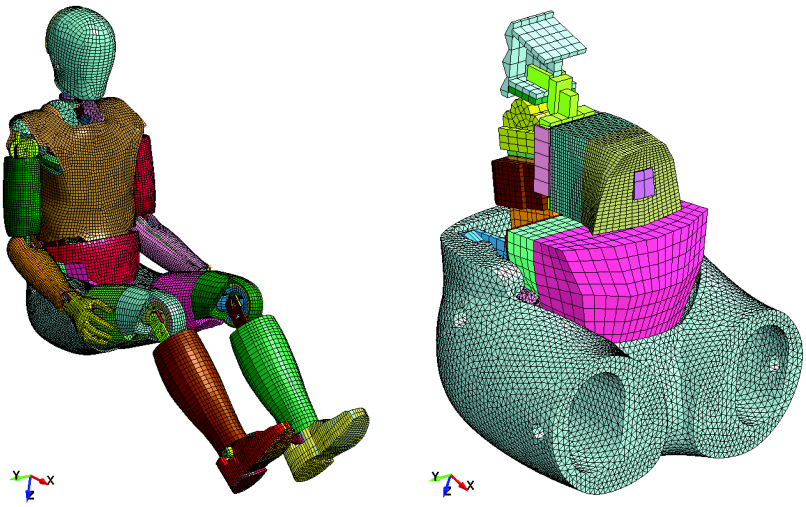

(a) Global view (b) Upper and lower abdomen

Figure 2.1 – THOR finite element model

1. Vehicle Research and Test Center
2. Finite Element
3. Computer-Aided Design

part	type	material model	density (kg m^{-3})	mass (g)
pelvis foam	volumetric	hyperelastic compressible (`MAT_083`)	199	2154
pelvis skin	shell	elastic (`MAT_001`)	940	1790
upper rear foam	volumetric	hyperelastic compressible (`MAT_083`)	1500	808
upper front foam	volumetric	hyperelastic compressible (`MAT_083`)	1500	764
lower rear foam	volumetric	hyperelastic compressible (`MAT_057`)	140	132
lower front foam	volumetric	hyperelastic compressible (`MAT_057`)	150	288
lower jacket	shell	hyperelastic incompressible (`MAT_181`)	160	46

Table 2.1 – THOR abdomen model parts list

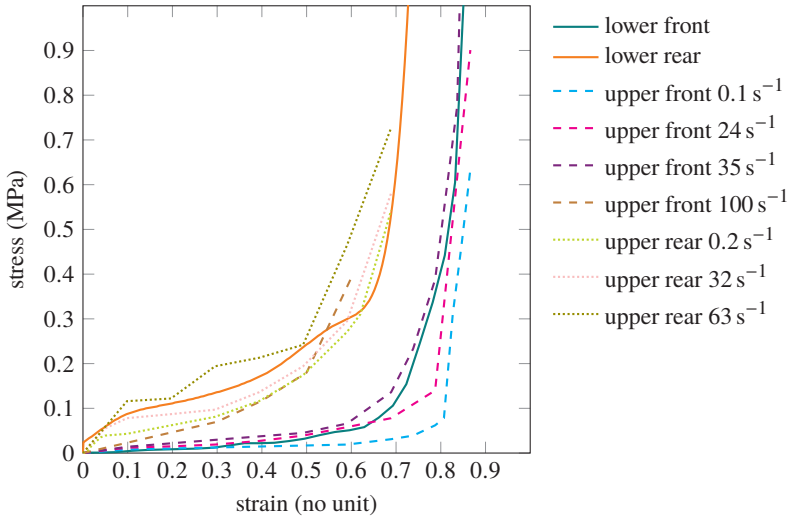

Figure 2.2 – Material curves for the foam parts of THOR abdomen

2.2.1 Evaluation

The component-level response of the dummy has been evaluated in THOR FE Manual (Panzer et al. 2015) according the the procedures detailed in THOR Certification Manual (NHTSA / GESAC, Inc. 2005a) and sled tests performed at 11 m s^{-1} with a 16 g's deceleration peak (protocol from Untaroiu et al. 2009). For the global evaluation, the belt forces, landmarks trajectories and kinematics, neck load cells signals and femur forces were in fair adequation with the test data.

However, regarding the component level evaluation, the upper and lower abdomen responses showed margin for improvement. Figure 2.3a shows the upper abdomen validation under a 8 m s^{-1} impact with a 18 kg wheel shaped impactor according to Nusholtz and Kaiker 1994 and Figure 2.3b shows the lower abdomen validation under a 6.1 m s^{-1} impact with a 32 kg impactor according to Cavanaugh et al. 1986. The response of the FE model shows a higher force response than the test data for both abdomen regions. This is believed to be due to imprecisions in the material characterisation for the abdomen foams and the pelvis.

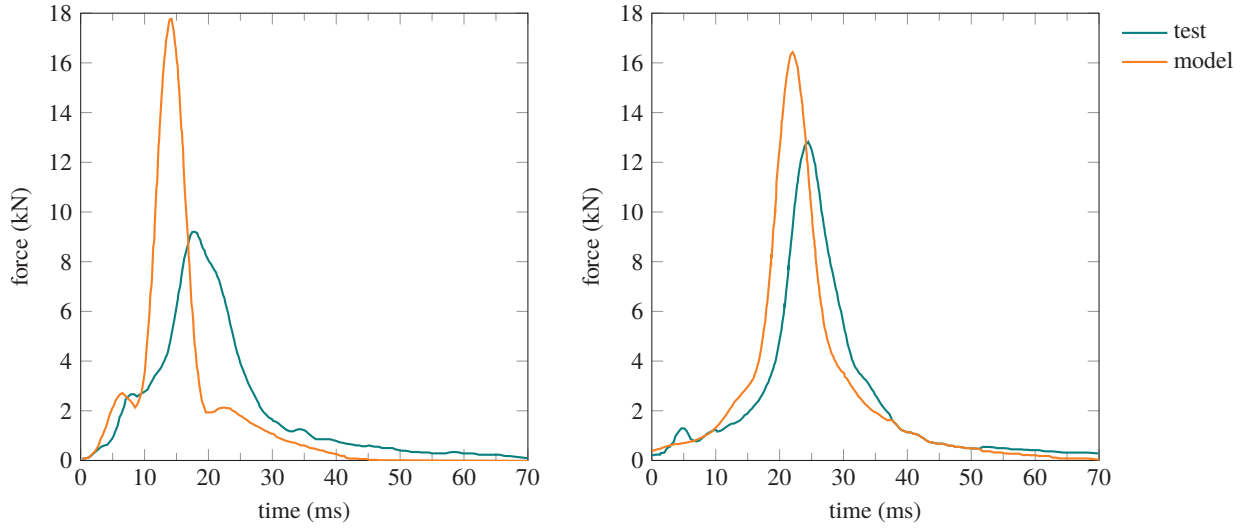

(a) Upper abdomen (b) Lower abdomen

Figure 2.3 – THOR finite element model abdomen validation (THOR FE Manual, Panzer et al. 2015)

2.2.2 Improvements

Improvements to the material properties of the THOR dummy model were performed as part of this work. The stress values of the pelvis material curves were multiplied by 0.16 according to tests performed by Toyota Motor Corporation and the front foam material properties have been re-characterised as part of this work to introduce material strain rate effect, the front foam being the part that influences the most the lower abdomen response. Drop tests were performed on cubic foam samples by by Toyota Motor Europe at strain rates from $6 \times 10^{-4}\,\mathrm{s}^{-1}$ to $120\,\mathrm{s}^{-1}$. The original material model was a simplified hyperelastic foam model (`MAT_057: LOW_DENSITY_FOAM`) and was replaced by a rate dependent hyperelastic foam model (`MAT_083: FU_CHANG_FOAM`) with new tabulated curves for different strain rates as seen on Figure 2.4.

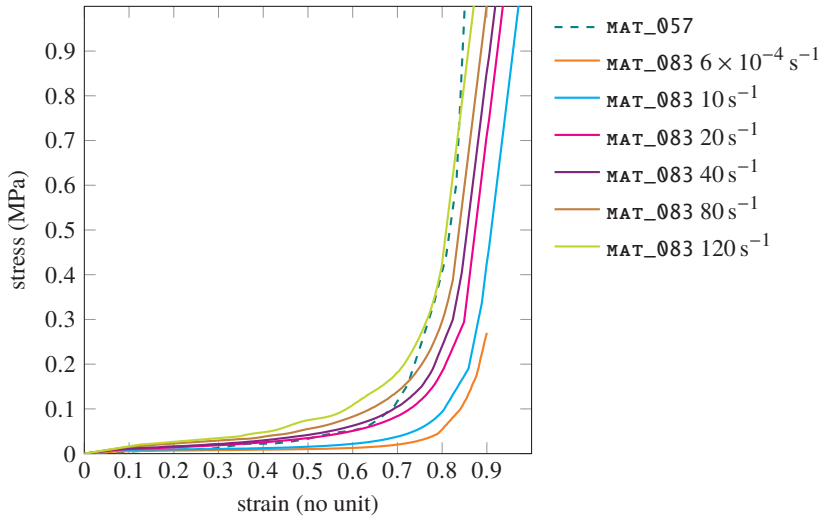

Figure 2.4 – New material curves for the front foam part of the lower abdomen

The modified dummy model has been validated using tests performed by NHTSA's VRTC and provided for this project. Two conditions were performed: a seatbelt loading reproducing the PMHS tests from Hardy et al. 2001 and an impactor loading reproducing the PMHS tests from Cavanaugh et al. 1986. For the seatbelt condition, the belt was pulled at the back of the dummy

by a pneumatic system, the dummy back being free. Figure2.5 shows the two different set-ups. Three different pressures were applied to the belt retraction system: 4.5 bar, 5.5 bar and 6.6 bar. The 6.6 bar condition corresponds to the loading applied to PMHS in Hardy et al. 2001. Figure 2.6a shows the different belt retraction profiles. For the impactor case, a 32 kg mass (diameter 25 mm) stroke the dummy with an initial velocity of 6.1 m s^{-1}.

In the simulations, the dummy was positioned seated according to the physical test and gravity was applied for 500 ms in order to obtain the initial geometry for the simulations. Initial stresses and strains resulting from the gravity deformation were not taken into account. Figure 2.7 shows the positioning and gravity deformation process. A fixed timestep of 4×10^{-4} ms was achieved through mass scaling.

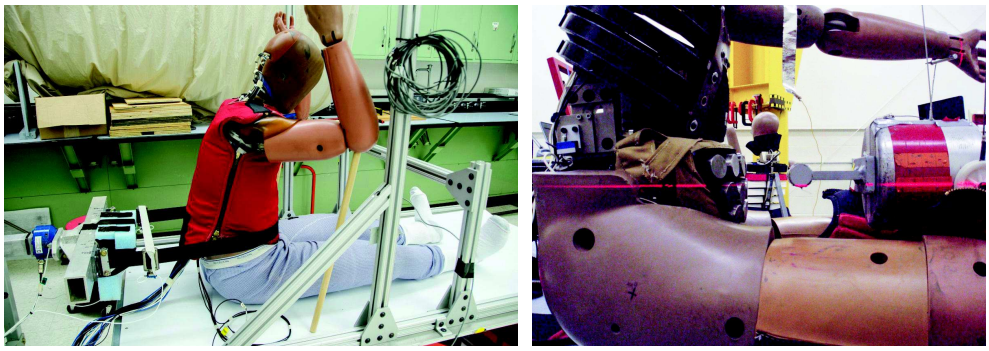

(a) Seatbelt (b) Impactor

Figure 2.5 – Test set-ups from VRTC

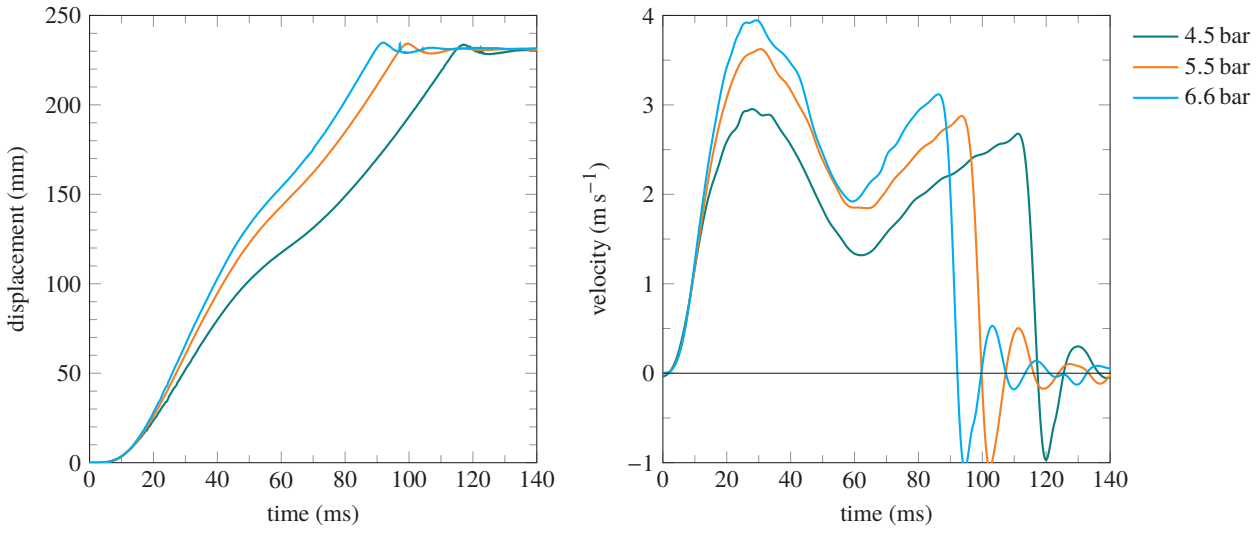

(a) Belt retraction (b) Belt retraction velocity

Figure 2.6 – Belt retraction velocity profiles from VRTC test data

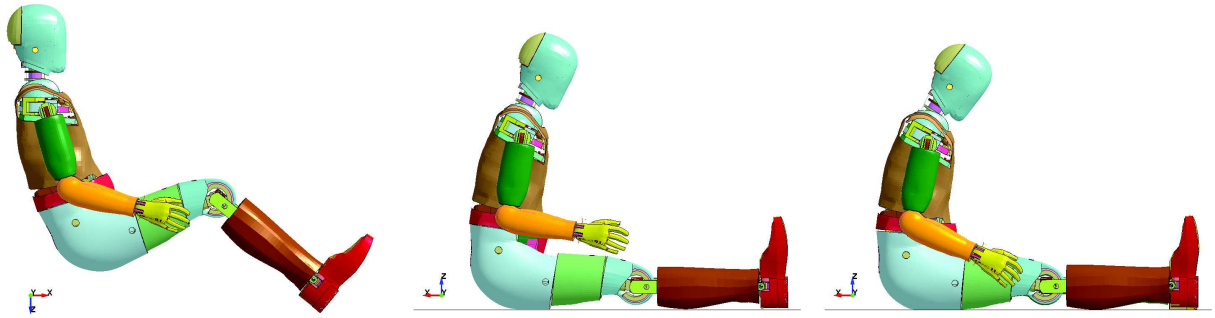

(a) Initial model (b) Before gravity deformation (c) After gravity deformation

Figure 2.7 – Positioning and gravity deformation

2.2.2.1 Seatbelt condition

The seatbelt conditions having a similar input profile, the dummy model response will be considered under the 6.6 bar condition since the standard dummy abdomen has only been tested under this condition. The results are presented on Figure 2.8. The belt retraction over time from test data was applied to the model, the back of the dummy being unrestrained. This condition corresponds to a 6.6 bar pressure applied to the belt retraction system. The model predicts well the response from test data, although there is a second force peak from the test data, that is not entirely reproduced by the simulation. But the second peak in the simulation is due to the seatbelt almost sliding over the pelvis, which is not the same phenomenon as in the test. Figure 2.9 shows the deformed shape of the model for different simulation times.

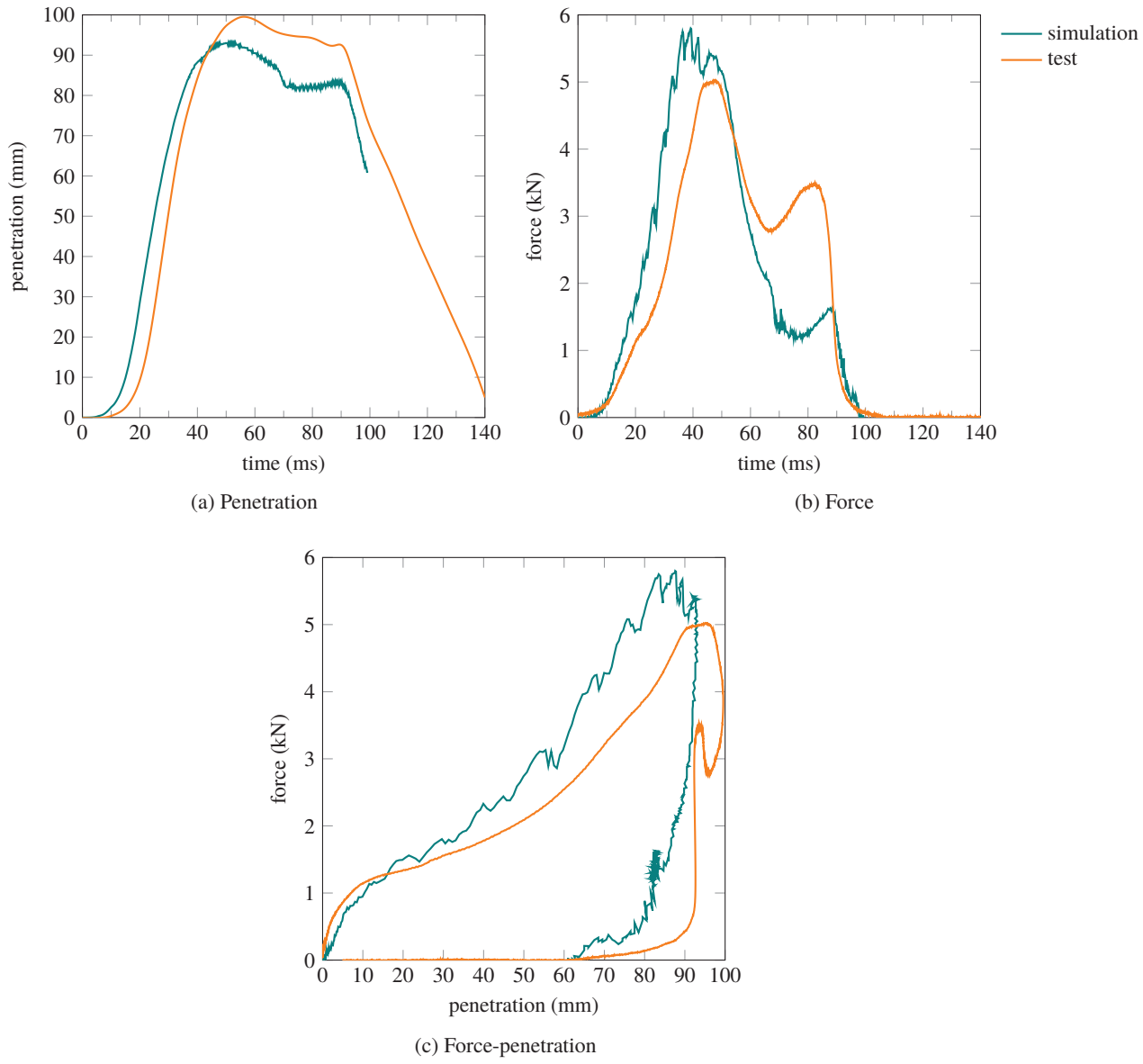

(a) Penetration

(b) Force

(c) Force-penetration

Figure 2.8 – THOR Mod-Kit response under Hardy et al. 2001 6.6 bar seatbelt loading

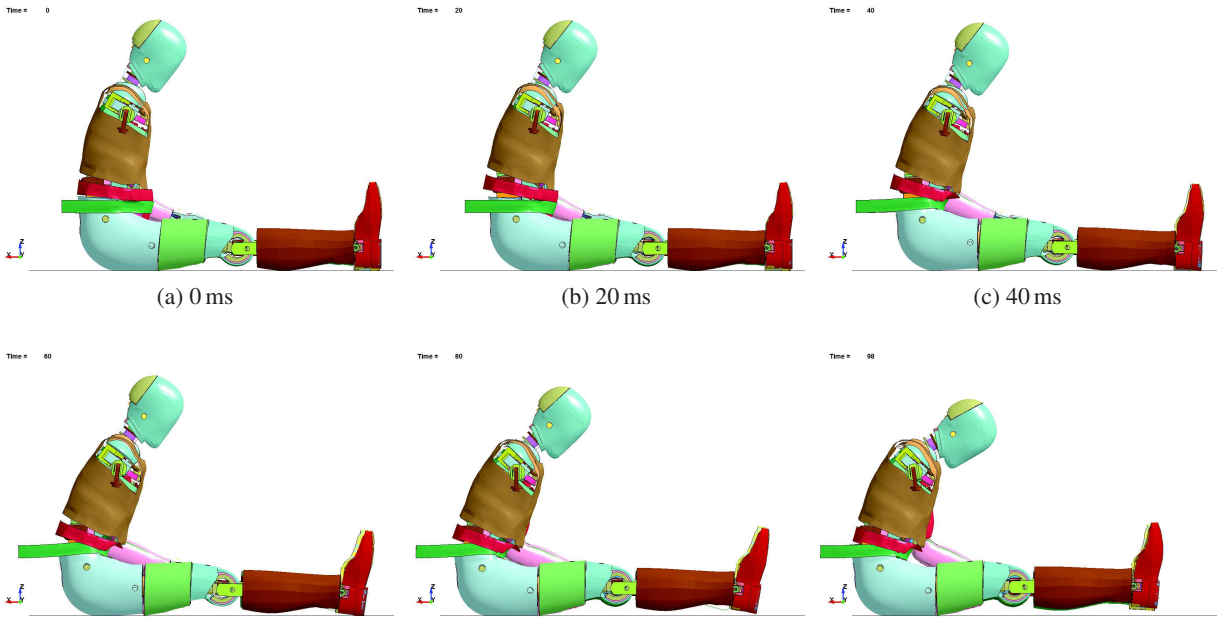

(a) 0 ms (b) 20 ms (c) 40 ms

(d) 60 ms (e) 80 ms (f) 98 ms

Figure 2.9 – THOR Mod-Kit deformed shape under Hardy et al. 2001 6.6 bar seatbelt loading
The right arm of the dummy has been blanked

2.2.2.2 Impactor condition

The dummy model response under impactor condition can be seen on Figure 2.10. The test data were not available over time, only as force / penetration graph. The force from the simulation was filtered at CFC [4] 180, the same way as the test data, which reduced the observed force peak. However the simulation results show a too high force and less penetration compared to the test data. The higher peak force is due to the abdomen foams being fully compressed and the impactor contacting the abdomen plate as it can been seen on Figure 2.10c. Here the test on the physical dummy is not properly reproduced by yhe model in terms of dummy behaviour. Figure 2.11 shows the model deformed shape along the simulation.

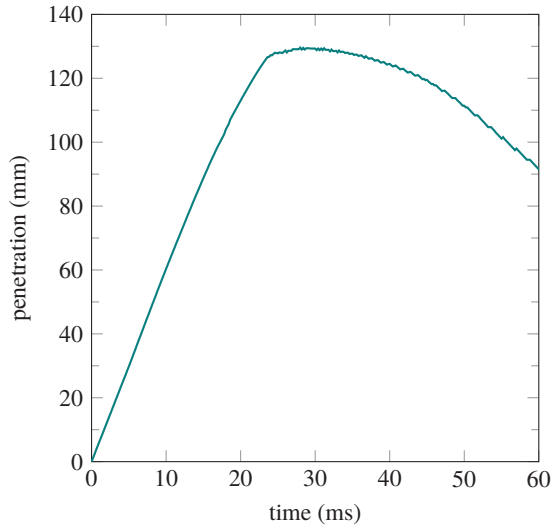

(a) Penetration

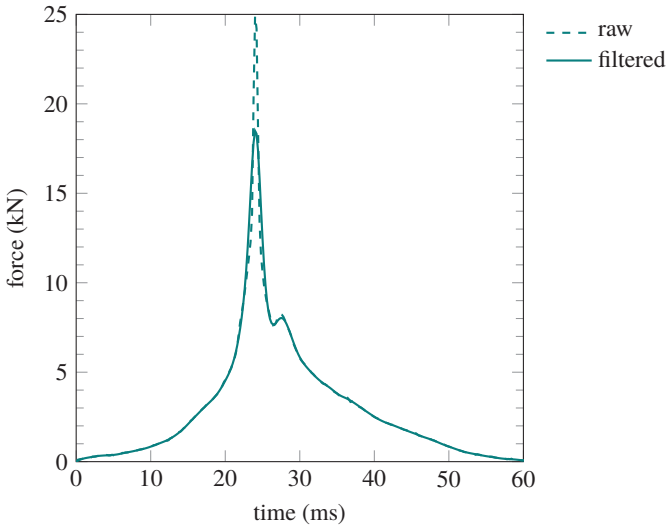

(b) Force

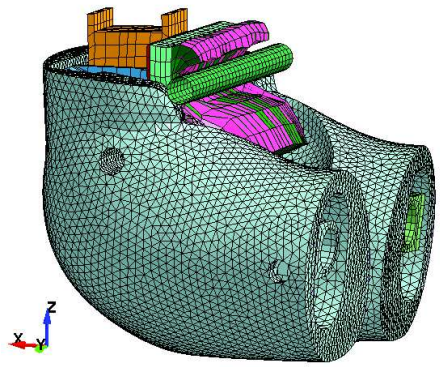

(c) Abdomen at 24 ms (jacket part hidden)

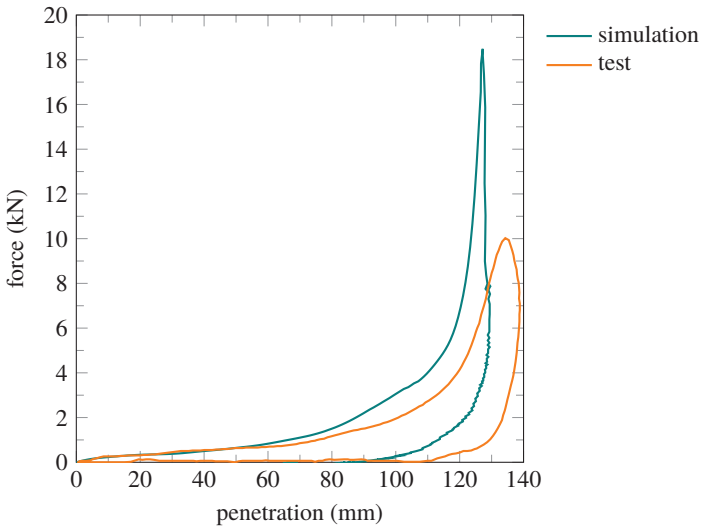

(d) Force-penetration

Figure 2.10 – THOR Mod-Kit response under impactor loading

4. Channel Frequency Class

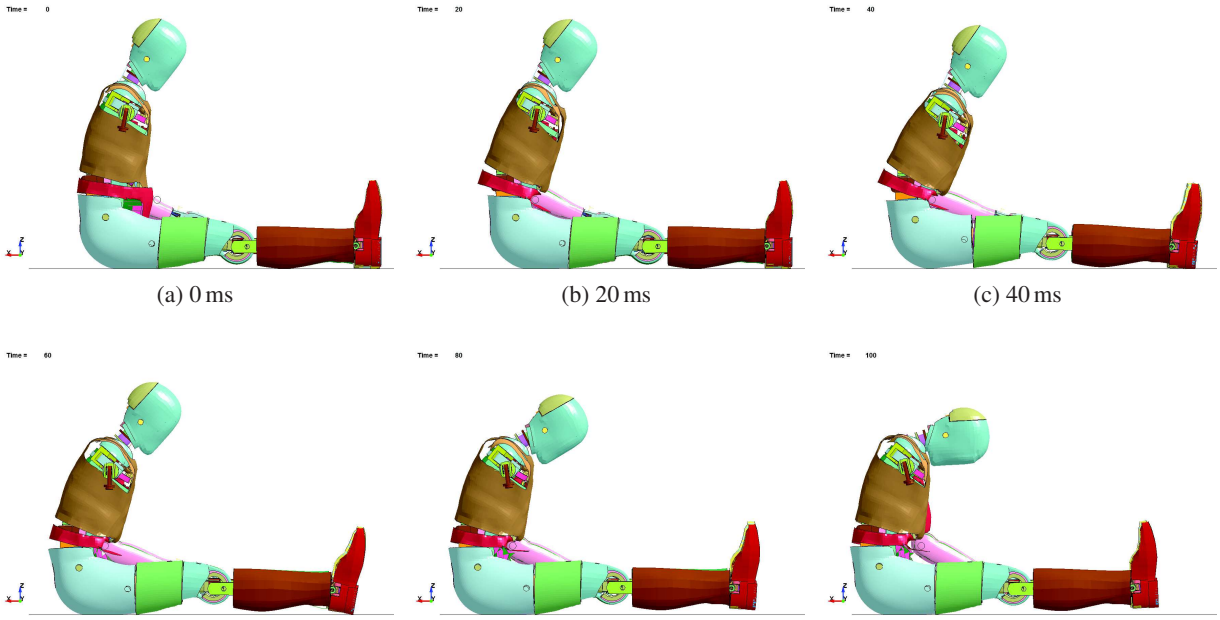

(a) 0 ms (b) 20 ms (c) 40 ms

(d) 60 ms (e) 80 ms (f) 100 ms

Figure 2.11 – THOR Mod-Kit deformed shape under impactor loading
The right arm of the dummy has been blanked

2.3 Development of prototype abdomen finite element model

2.3.1 Prototype description

The prototype abdomen developed for the THOR dummy by IFSTTAR and Toyota Motor Europe is a modification of the dummy standard abdomen. DGSP sensors were removed and replaced by two APTS sensors placed in vertical position thanks to holes drilled in the front foam part as described in Compigne et al. 2015. The APTS sensors (presented in Beillas et al. 2012) consist in a 50 mm diameter polyurethane bladder filled with paraffin oil and equipped with a pressure sensor. In order to increase the initial inertia response of the abdomen, 825 g of additional mass were added through the attachment of fifteen steel cylinders attached to the fabric bag of the dummy abdomen by a Velcro layer. Figure 2.12 shows the APTS sensors and the prototype abdomen.

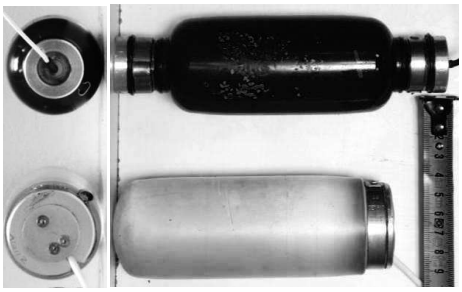

(a) APTS sensors (Beillas et al. 2012)

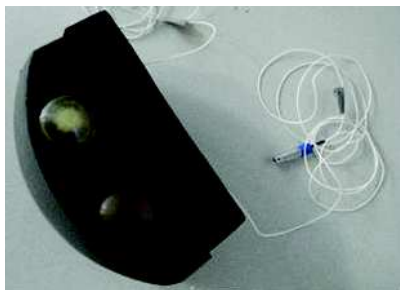

(b) Prototype abdomen

(c) Abdomen with additional masses

Figure 2.12 – IFSTTAR / Toyota Motor Europe prototype abdomen

2.3.2 Model development

The model of the standard dummy was modified to include the model of the prototype abdomen. The APTS polyurethane bladders were modelled as an elastic material with an 3.25 MPa Young's modulus and a 0.38 Poisson's ratio. The APTS fluid is modelled with a solid material but includes an equation of state with only one coefficient which gives a relationship between the pressure in the material (P) and the current volume of the material (V) as described by Equation 2.1. This modelling method for this kind of structure have been described in Soni and Beillas 2015. C_1 is equal to 0.5 GPa in the model. A viscosity coefficient of 785 Pa s is also defined. The fifteen steel cylinders were modelled by shell elements and each of them is rigidly linked to shell elements of the front foam coat. The front and rear foams meshes have been refined as shown on Figure 2.13 in order to have a element size of around 5 mm instead of between 10 mm and 15 mm previously. Table 2.2 gives a list of the prototype abdomen model parts.

The APTS sensors FE model provided by IFSTTAR had been previously validated under compression by a 50 mm diameter impactor with a 1 m s^{-1} velocity until 50 % compression (25 mm). However, in simulation the sensors are compressed more than 50 %. Figure 2.14 shows that the model predicts perfectly the sensors response in terms of pressure measurement but predicts a force a bit lower than the test data. This is probably due to the fact that the fluid (little compressibility) was modelled with a compressible material.

The APTS model was inserted in the front foam part of the THOR model prior to applying gravity for 500 ms to the full dummy. The abdomen internal plate served as reference to position the new abdomen. Care has been taken that the APTS do not penetrate neither the pelvis parts nor the upper abdomen before applying gravity. The vertical position of the APTS in the abdomen has therefore been adjusted in order not to penetrate the pelvis and the dummy torso has been rotated in order not to have initial penetrations between the upper abdomen and the APTS.

$$P = C_1 \cdot \frac{V_0 - V}{V} \tag{2.1}$$

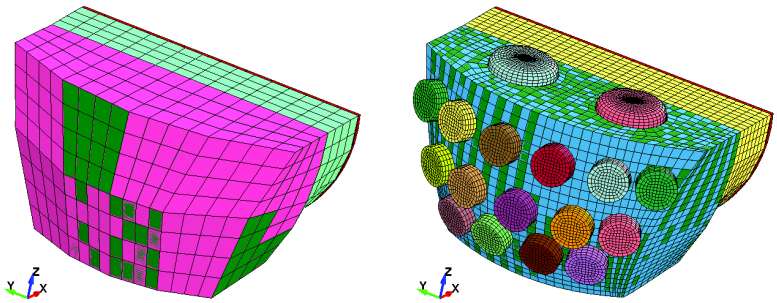

(a) Standard abdomen (b) Prototype abdomen

Figure 2.13 – Standard and prototype abdomen models

part	type	material model	density (kg m^{-3})	mass (g)
APTS right bladder	volumetric	elastic (MAT_001)	1400	119
APTS left bladder				
APTS right fluid	volumetric	equation of state (MAT_009)	865	148
APTS left fluid				
APTS right cap	volumetric	rigid (MAT_020)	2700	45
APTS left cap				
15 steel cylinders	shell	rigid (MAT_020)	2700	825 for the 15 cylinders using added mass

Table 2.2 – Prototype abdomen model parts list

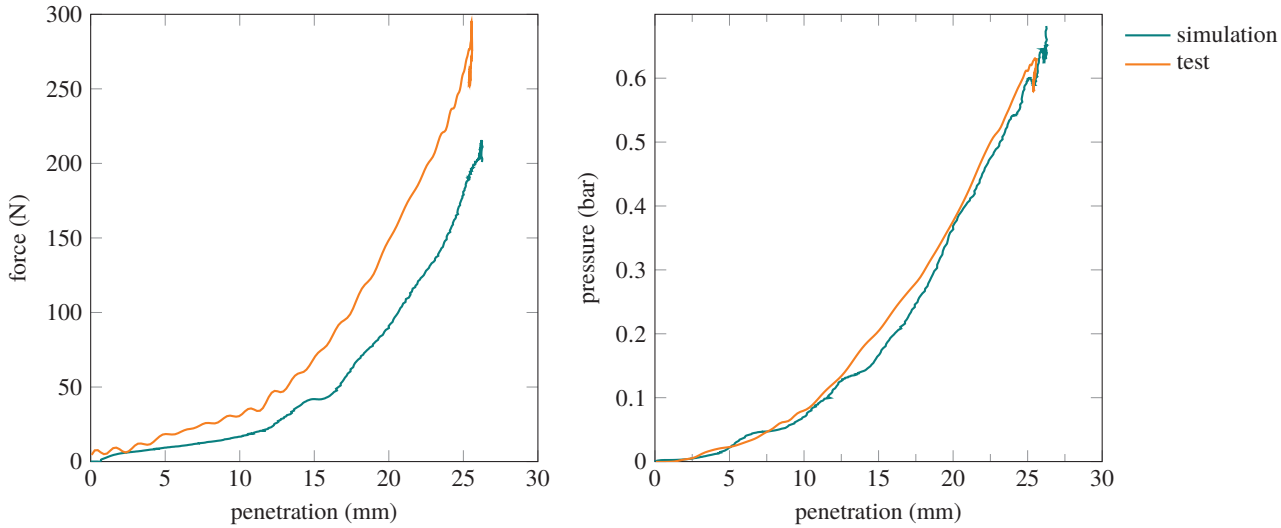

(a) Force-penetration

(b) Pressure-penetration

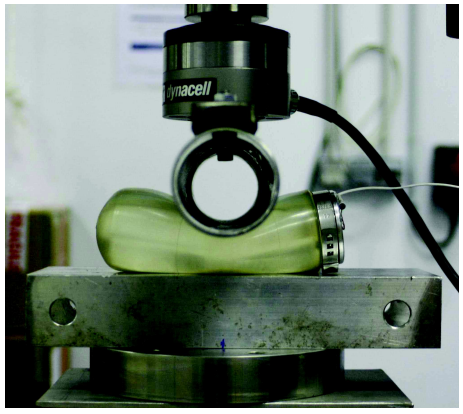

(c) Compression test

Figure 2.14 – APTS compression test

Force and pressure signals from simulation were filtered with a CFC 180 filter

2.3.3 Evaluation

The abdomen model of the prototype abdomen was evaluated versus test on the physical dummy performed under the conditions described in Section 2.2.2.

2.3.3.1 Seatbelt simulations

Figure 2.15 shows the results of simulation for the 6.6 bar pressure condition. In addition to the force and penetration results, Figure 2.15c compares the pressure measured in the APTS sensors and the simulation prediction. Two curves for the same case (test or simulation) represent the left and right sensor response. The model reproduces well the test data in terms of shape although the penetration and force peak values are slightly overestimated. The force unloading response is also not well reproduced

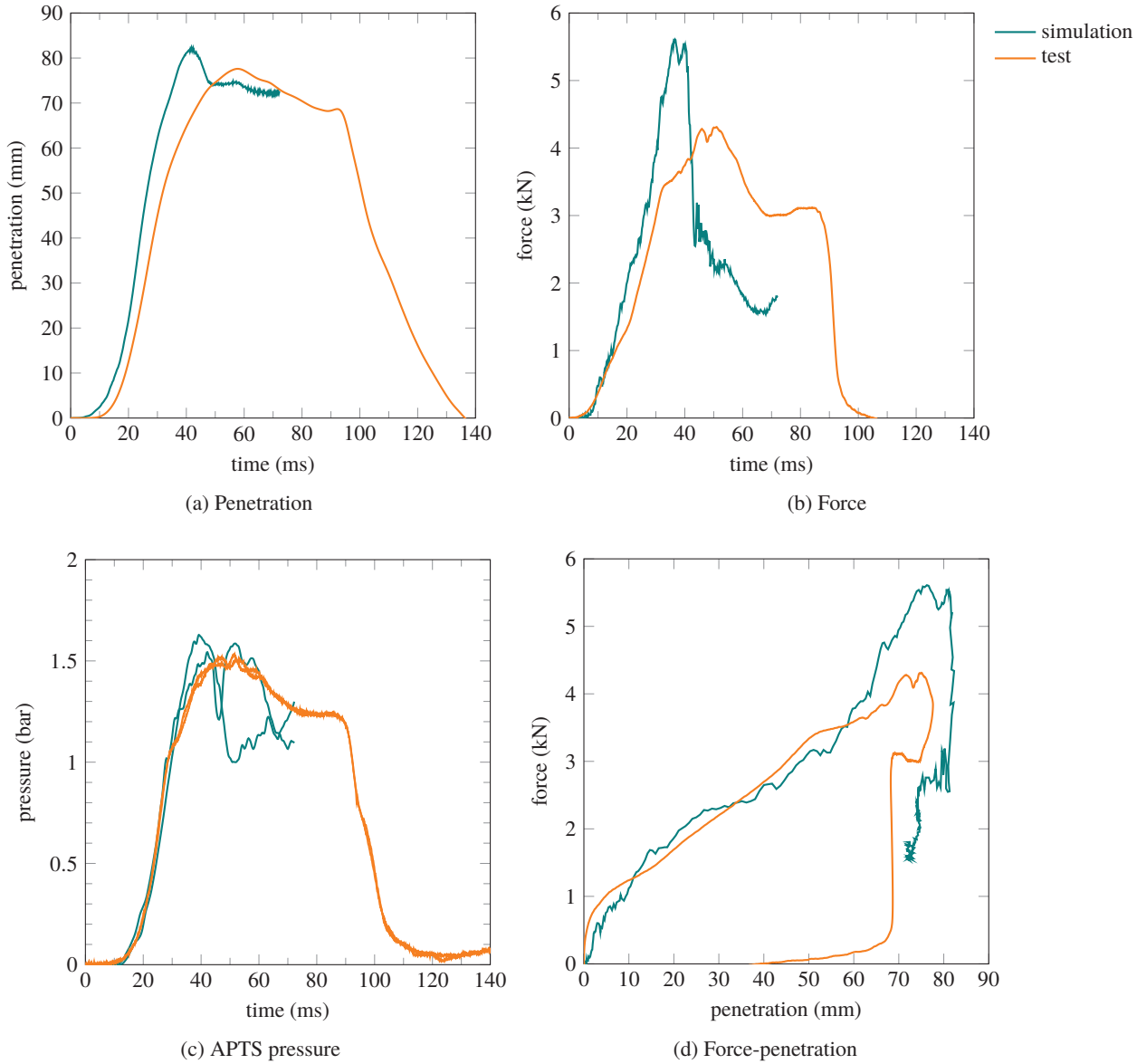

(a) Penetration

(b) Force

(c) APTS pressure

(d) Force-penetration

Figure 2.15 – THOR dummy with prototype abdomen response under Hardy et al. 2001 6.6 bar seatbelt loading

Pressure signals filtered with CFC 180 filter

2.3.3.2 Impactor simulations

Impactor simulations with a 6.1 m s^{-1} velocity created negative volumes in the APTS fluid, leading to an early termination. A maximum termination time of 24 ms could be reached. The results of the simulation of impactor test are presented on Figure 2.16. Although the simulation terminates early, there is a good adequation between the test and simulation results, except from pressure which is lower in the simulation. The early oscillations in the force signal are due to the contact between rigid parts: the impactor and the added masses in front of the abdomen. Although separated from each other by the jacket, the contact between rigid parts with a high initial velocity creates oscillations due to the high stiffness of the virtual springs used to compute the contact force.

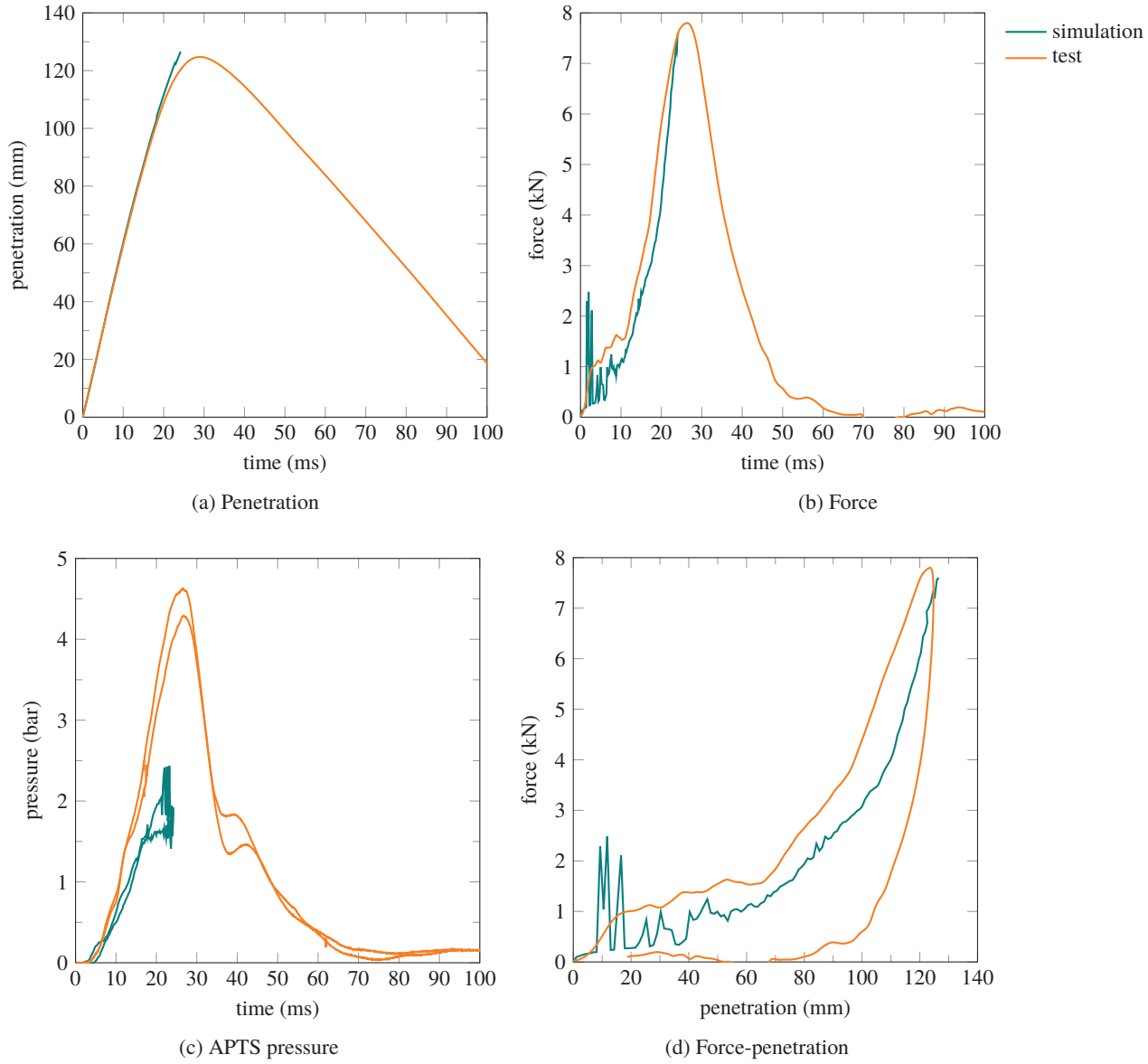

(a) Penetration

(b) Force

(c) APTS pressure

(d) Force-penetration

Figure 2.16 – THOR dummy with prototype abdomen response under impactor loading

2.4 Conclusion

The finite element model of the THOR dummy provided by NHTSA has been improved in order to have a model response correlating better with the test data. Based on these improvements, the abdomen prototype finite element model has been included in the dummy finite element model. This new model allows to reproduce the prototype abdomen response under seatbelt and impactor test. The simulation results do not match perfectly the test data, it appears that the model reproduces better a loading of the abdomen by a seatbelt compared to an impactor loading. This is true for the standard abdomen response and for the prototype abdomen pressure prediction. The seatbelt loading being a more frequent case of abdomen loading considering a car crash, this test case is a better candidate for injury prediction with the dummy model.

Chapter 3

THOR abdomen prototype improvements

Contents

3.1 Introduction

The finite element model of the THOR dummy with the IFSTTAR / Toyota prototype abdomen have been developed in the previous chapter. The aim of this chapter is to analyse the mechanical behaviour of the dummy abdomen under impact in order to draw ways of improvement. This has been done in subcomponent tests (loading of the dummy abdomen only) with a simplified mechanical model and with the prototype FE model. Sled test simulations have also been performed with the dummy FE model in order to study the influence of the prototype abdomen on the dummy kinematics in a loading case representative of a crash.

3.2 Subcomponent tests

3.2.1 Lumped element model

A simplified model of the human abdomen was built to reproduce dynamic loading tests on the human abdomen and on the THOR dummy abdomen. The aim of this lumped element model is to determine the main characteristics of the human abdomen response under impact and to improve the biofidelity of the THOR dummy abdomen.

3.2.1.1 Previous models

A lumped element model was proposed in Trosseille et al. 2002 where the abdomen was approximated by a spring in parallel with a damper to simulate a seatbelt test (see Figure 3.1a). This was representing the contribution of a static and a dynamic force to the abdomen response. The abdomen force was computed from the test penetration and penetration velocity data with the relationship $F = K \cdot x + C \cdot \dot{x}$. The parameters were identified from test data using an analytical method.

Trosseille et al. 2002 also developed a lumped element model applied to the THOR dummy. A mass M was added at the front of the model used for the PMHS subjects and a non-linear spring was used giving an $F = K_0 \cdot \dfrac{L}{L - x} \cdot x$ contribution, L being the thickness of the foam layers of the dummy abdomen. The parameters identified for the PMHS subjects were on average $K = 12\,850\,\mathrm{N\,m^{-1}}$ for the stiffness contribution and $C = 765\,\mathrm{N\,m^{-1}\,s}$ for the damping contribution. For the THOR dummy, L was set to 0.12 m and the average parameters were $M = 0.15\,\mathrm{kg}$, $K_0 = 11\,225\,\mathrm{N\,m^{-1}}$ and $C = 193\,\mathrm{N\,m^{-1}\,s}$. Figure 3.2 shows the validation of the model versus THOR and PMHS data.

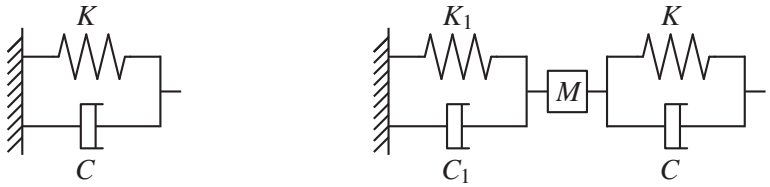

(a) Trosseille et al. 2002 (b) Lamielle et al. 2008

Figure 3.1 – Previous lumped element models for the abdomen

In Lamielle et al. 2008 seatbelt tests, the use of force sensors between the back of the subject and the testing apparatus allowed a more detailed modelling consisting in two spring / damper models in series with a mass in between (see Figure 3.1b). The model parameters were identified from

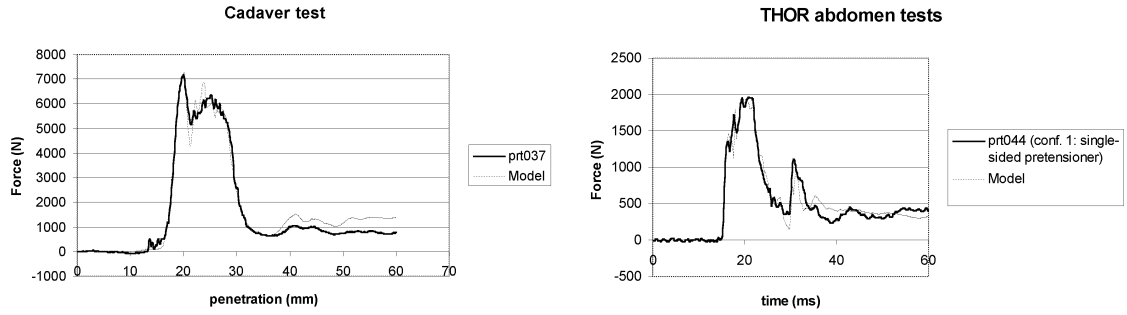

(a) Versus PMHS (b) Versus THOR

Figure 3.2 – Validation of model from Trosseille et al. 2002

test data with a similar method as in Trosseille et al. 2002. Then the resolution of the model was performed with a 4th order Runge-Kutta method having the abdomen force from test data imposed. The belt displacement and velocity were then compared to test data.

The parameter K_1 was identified first in a F_{back} versus x_1 diagram by fitting a cubic curve ($F_{\text{back}} = K_1 \cdot x_1^3$) through the point $\left(\left(x_1^{\max}\right)^3 ; F_{\text{back}}\left(\left(x_1^{\max}\right)^3\right)\right)$. The measured F_{back} data had been scaled before with a factor comprised between 0.8 and 1.2 in order to have a force equal to zero after the unloading . C_1 was then determined for each test fitting a cubic curve in a $F_{\text{back}} - K_1 \cdot x_1^3$ versus $\dot{x}_1$ diagram. However, the determination of K_1 does not take into account the contribution of C_1 to F_{back}. The parameters K and C were determined in a similar way for each test. The same remark can be expressed that the determination of K does not take into account the contribution of C to the force F.

The average parameters found for the first block of the model representing the part of the abdomen between the front wall and the centre of gravity were $K = 13\,000\,\text{kN m}^{-3}$ and $C = 665\,\text{N m}^{-1}\,\text{s}$. The mass representing the abdomen was chosen as $M = 14\,\text{kg}$. The second block was showing much more stiffness with $K_1 = 800\,000\,\text{kN m}^{-3}$ and $C_1 = 3940\,\text{N m}^{-3}\,\text{s}^3$. The components K, K_1 and C_1 were non linear components with a cubic relationship, for instance $F = K \cdot x^3$. Similarly, $F = K_1 \cdot x^3$ and $F = C_1 \cdot \dot{x}^3$ in the other components. But $F = C \cdot \dot{x}$ for the C component. Figure 3.3 shows the validation of those models versus PMHS data.

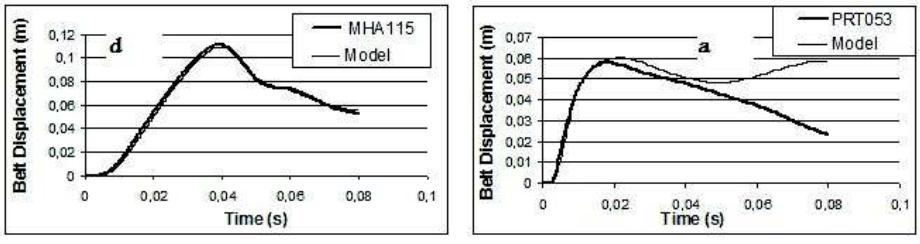

(a) Versus MHA data (b) Versus PRT data

Figure 3.3 – Validation of model from Lamielle et al. 2008

A thorax model for an impactor test was developed in Lobdell et al. 1973, consisting of a mass representing the impactor (m_1), a mass representing the sternum, the ribs and the thoracic content (m_2) and a mass representing the spine (m_3). These masses are linked by the spring k_{12} representing the thorax skin and a block of springs and dampers representing the ribcage and the thoracic content. The components are linear except k_{23} that is bi-linear in order to match the target corridors for large deflections and c_{23} that has different damping values for tension and compression in order to model force decay. The initial velocity of the impactor was applied as input condition of the model. Figure 3.4a shows the models. The resolution of the system's equations was performed until the